Inorganic Chemistry
Article

Inorg. Chem. **2009**, *48*, 8729–8735 **8729**
DOI: 10.1021/ic900826q

Pathways of Water Oxidation Catalyzed by Ruthenium "Blue Dimers" Characterized by ^{18}O-Isotopic Labeling

Jonathan L. Cape, William F. Siems, and James K. Hurst*

Department of Chemistry, Washington State University, Pullman, Washington 99164-4630

Received April 28, 2009

Earlier $^{18}O-H_2O$ labeling studies had indicated that two concurrent pathways may exist for water oxidation catalyzed by $[Ru(bpy)_2(OH_2)]_2O^{4+}$, a μ-oxo bridged diruthenium complex known colloquially as the "blue dimer". Specifically, the distribution of O_2 isotopomers obtained following its generation by the catalytically active form, $[Ru(bpy)_2(O)]_2^{4+}$, suggested pathways in which either (1) one O atom was obtained from the terminally coordinated oxo atom and the second from the solvent or (2) both O atoms were obtained from the solvent. Plausible mechanisms have been advanced for the former pathway, but the second is enigmatic. In the present study, experiments are described that eliminate possibilities that the second pathway arises artifactually from rapid water exchange in reactive intermediary oxidation states of the catalyst, by mechanisms involving scrambling of the O_2 that is formed during reaction, or by mechanisms involving participation of the oxidant (Ce^{4+} or $S_2O_8^{2-}$). Comparative studies of partitioning between the two pathways made using catalysts containing substituted bipyridine ligands are consistent with a previously proposed pathway that involves noninnocent participation of these ligands.

Introduction

Development of catalysts capable of oxidizing water on a sustained basis may be crucial to achieving technological goals in direct solar photoconversion to fuels, which requires the availability of a plentiful and inexpensive source of reducing equivalents. Largely in response to this projected need, inorganic chemists have sought to identify the complex underlying reaction mechanisms of existing catalysts as a means of directing the conceptual design of new generations of superior catalysts. The catalysts that have been most extensively studied from this perspective are μ-oxo dimeric ruthenium coordination complexes with the general formula *cis*,*cis*-$[Ru^{III}L_2(OH_2)]_2O^{n+}$ (denoted hereafter {**3**,**3**}),[1] where L is 2,2′-bipyridine or a ring-substituted analog.[2,3] Although water oxidation by these ions is incompletely understood, there is general consensus that the catalytically active species are the corresponding $[RuL_2(O)]_2O^{n+}$ ions ({**5**,**5**}) formed by four-electron oxidation of {**3**,**3**}, which undergo first-order decay with the release of O_2.[4−7] Among the various measurements made on these ions, ^{18}O-isotope labeling studies have been particularly informative. Selective labeling of the bridging oxo atom in $[Ru^{III}L_2(OH_2)]_2O^{n+}$ has shown unequivocally that it does not participate in O_2 formation,[7,8] whereas labeling at the terminal aqua (oxo) positions has revealed two distinct pathways leading to O_2 formation.[5] Specifically, for one of the pathways (denoted EN in Scheme 1), one O atom is obtained from the coordination sphere and the other from the solvent; for the other pathway (denoted S_2 in Scheme 1), both O atoms are obtained from the solvent. There is no evidence supporting a pathway in which both O atoms are obtained from the coordination sphere, that is, by either bimolecular reactions between two complex ions or unimolecular coupling of bound ruthenyl oxo atoms with reductive elimination of O_2 (denoted RE in Scheme 1).

We have proposed that the EN pathway involves the concerted addition of H_2O across the ruthenyl oxo atoms to give the transitory peroxo-bound species, $[(bpy)_2Ru(OOH)ORu(OH)(bpy)_2]^{4+}$;[5] this suggestion has received theoretical support in the form of DFT calculations, for which a detailed reaction coordinate was calculated.[9] The

*To whom correspondence should be addressed. Tel.: 509-335-7848. Fax: 509-335-8867. E-mail: hurst@wsu.edu.

(1) The notation used is intended to indicate the overall level of oxidation of the complex, which may not represent the electronic distribution within the dinuclear core. For example, {**5**,**5**}, formally $[(bpy)_2Ru^{V}(=O)]_2O^{4+}$, is suggested from DFT calculations to have an electronic distribution corresponding to a dioxo radicaloid species,[9] i.e., $[(bpy)_2Ru^{IV}(-O^{\bullet})]_2O^{4+}$, for which each terminal oxo is formally assigned a value of −1, rather than −2.

(2) Liu, F.; Concepcion, J. J.; Jurss, J. W.; Cardolaccia, T.; Templeton, J. L.; Meyer, T. J. *Inorg. Chem.* **2008**, *47*, 1727–1752.
(3) Hurst, J. K.; Cape, J. L.; Clark, A. E.; Das, S.; Qin, C. *Inorg. Chem.* **2008**, *47*, 1753–1764.
(4) Lei, Y.; Hurst, J. K. *Inorg. Chim. Acta* **1994**, *226*, 179–185.
(5) Yamada, H.; Siems, W. F.; Koike, T.; Hurst, J. K. *J. Am. Chem. Soc.* **2004**, *126*, 9786–9795.
(6) Binstead, R. A.; Chronister, C. W.; Ni, J.; Hartshorn, C. M.; Meyer, T. J. *J. Am. Chem. Soc.* **2000**, *122*, 8464–8473.
(7) Yamada, H.; Hurst, J. K. *J. Am. Chem. Soc.* **2000**, *122*, 5303–5311.
(8) Lei, Y.; Hurst, J. K. *Inorg. Chem.* **1994**, *33*, 4460–4467.
(9) Yang, X.; Baik, M.-H. *J. Am. Chem. Soc.* **2006**, *128*, 7476–7485.

Published on Web 08/19/2009

Scheme 1. Isotope-Defined Unimolecular Pathways for O_2 Formation

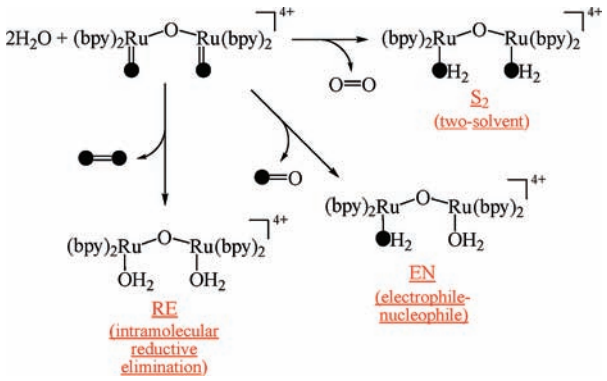

other pathway (S_2) is considerably more problematic because there is no obvious mechanism. Reactions involving dihydroperoxide[10] or bridging ozonide[11] intermediates have been suggested, but their formation appears to be energetically highly unfavorable.[5] An alternative mechanism that retains the notion of a concerted addition of a water molecule in the initial step can be invoked if one assumes noninnocent participation of the bipyridine ligands. This mechanism is based upon previous considerations of O_2 formation during alkaline decomposition of $Ru(bpy)_3^{3+}$[12−14] that, in turn, derive from well-established covalent hydration[15] and pseudobase-forming[16] reactions of nitrogen heterocycles. In the proposed mechanism (Figure 1), the incipient $OH^•$ fragment adds not to a terminal ruthenyl O atom of {**5**,**5**} but to the bipyridine ring, initiating a series of reactions leading ultimately to the formation of unstable dioxetanes that undergo internal rearrangement to {**3**,**3**} with the elimination of O_2.[5] Experimental data that are consistent with the initial steps of this mechanism include diagnostic near-infrared bands and electron paramagnetic resonance (EPR) signals whose dynamics correlate with O_2 evolution rates[14,17] and radiolysis studies demonstrating that OH^- uptake follows adduct formation between $OH^•$ and 2,2-bipyridine or $Ru(bpy)_3^{2+}$ in the presence of mild oxidants.[18] Nonetheless, there appear to be no well-established chemical precedents for the remaining steps, in particular, the internal redox reactions leading to O−O bond formation. Since support for this pathway rests entirely upon the isotope labeling results, it is critical to eliminate alternative mechanisms that might give artifactual formation of O_2 from two solvent molecules. In this study, we demonstrate that the data cannot be reconciled by mechanisms involving water exchange at the coordination site during turnover or by scrambling of the initially formed O_2 with solvent or coordinated O atoms. The general phenomenon of dual reaction pathways is extended to include several

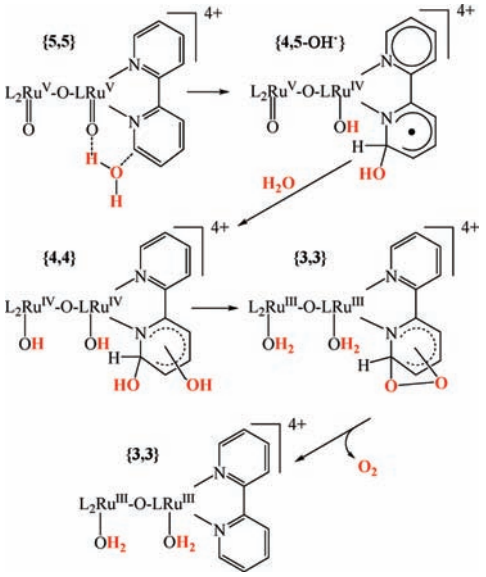

Figure 1. A hypothetical two-solvent pathway involving participation of bipyridine ligands. In the initial step, concerted addition of H_2O leads to formation of a bipyridine−$OH^•$ adduct. Subsequent one-electron internal oxidation of the adduct promotes the addition of a second H_2O to form a diol intermediate. This second addition need not be concerted but might proceed stepwise, for example, by internal proton-coupled electron transfer to Ru^V, followed by OH^- addition to the bipyridyl cation (see, e.g., Maliyackel, A. C.; Walz, W. L.; Lilie, J.; Woods, R. J. *Inorg. Chem.* **1990**, *29*, 340−348). Further two-electron oxidation of the diol gives a dioxetane, which undergoes elimination to give {**3**,**3**} and O_2. Sites of OH addition to the ring are deliberately unspecified in this drawing but, in principle, could occur at any of the carbon positions.

$[Ru^{III}L_2(OH_2)]_2O^{n+}$ analogs of {**3**,**3**} and to photoinitiated reactions involving {**3**,**3**}. These latter studies demonstrate that the isotopomer distribution is independent of the oxidant identity but dependent upon the identities of the bipyridine ligand ring substituents in a manner that is consistent with the proposed dual pathway model.

Experimental Section

Materials. The complex ions, *cis*,*cis*-$[Ru^{III}(bpy)_2(OH_2)]_2O^{4+}$,[7,19] *cis*,*cis*-$[Ru^{III}(4,4'\text{-dimethylbpy})_2(OH_2)]_2O^{4+}$,[7] *cis*,*cis*-$[Ru^{III}(5,5'\text{-dimethylbpy})_2(OH_2)]_2O^{4+}$,[7] and *cis*,*cis*-$[Ru^{III}(5,5'\text{-dicarboxybpy})_2(OH_2)]_2O^{4+}$[20] (bpy = 2,2′-bipyridine) were prepared essentially as described in the literature and isolated as their perchlorate salts. Isotopic enrichment of the aqua positions was achieved by incubating concentrated solutions of the ions in 95% [^{18}O]-H_2O (Cambridge Isotope Laboratories) that also contained sufficient trifluoromethanesulfonic (triflic) anhydride to give 0.5 M triflic acid; the dicarboxybpy analog was partially oxidized to {**3**,**4**} with Ce^{4+} during this exchange to increase its solubility. Under these conditions, water exchange on {**3**,**3**} occurs within several minutes.[21] Immediately before isotopic dilution into reaction media, the complexes were stoichiometrically oxidized to {**3**,**4**}, as monitored spectrophotometrically; water exchange occurs only very slowly ($t_{1/2} \geq 20$ h) in this oxidation state.[21] These procedures also do not lead to any exchange in the natural abundance bridging O atom.[7,8] The ligand 4,4′-dicarboxyethyl-2,2′-bipyridine (dcb) was prepared by the addition

(10) Hurst, J. K.; Zhou, J.; Lei, Y. *Inorg. Chem.* **1992**, *31*, 1010–1017.
(11) Meyer, T. J. In *Oxygen Complexes and Oxygen Activation by Transition Metals*; Martell, A. E., Sawyer, D. T., Eds.; Plenum Press: New York, 1988; pp 33−48.
(12) Ghosh, P. K.; Brunschwig, B. S.; Chou, M.; Creutz, C.; Sutin, N. *J. Am. Chem. Soc.* **1984**, *106*, 4722–4783.
(13) Ledney, M.; Dutta, P. *J. Am. Chem. Soc.* **1995**, *117*, 7687–7695.
(14) Hurst, J. K. *Coord. Chem. Rev.* **2005**, *249*, 313–328.
(15) Albert, A.; Armarego, W. L. F. *Adv. Heterocycl. Chem.* **1965**, *4*, 1–42. Albert, A. *Adv. Heterocycl. Chem.* **1976**, *20*, 117–143.
(16) Bunting, J. W. *Adv. Heterocycl. Chem.* **1979**, *25*, 1–82.
(17) Cape, J. L.; Hurst, J. K. *J. Am. Chem. Soc.* **2008**, *130*, 827–829.
(18) Creutz, C.; Sutin, N. *Proc. Natl. Acad. Sci. U.S.A.* **1975**, *72*, 2858–2862.
(19) Gilbert, J. W.; Eggleston, D. S.; Murphy, W. A., Jr.; Geselowitz, D. A.; Gersten, S. W.; Hodgson, D. J.; Meyer, T. J. *J. Am. Chem. Soc.* **1985**, *107*, 3855–3864.
(20) Rotzinger, F. P.; Munavalli, S.; Comte, P.; Hurst, J. K.; Grätzel, M.; Pern, F.-J.; Frank, A. J. *J. Am. Chem. Soc.* **1987**, *109*, 6619–6626.
(21) Yamada, H.; Koike, T.; Hurst, J. K. *J. Am. Chem. Soc.* **2001**, *123*, 12775–12780.

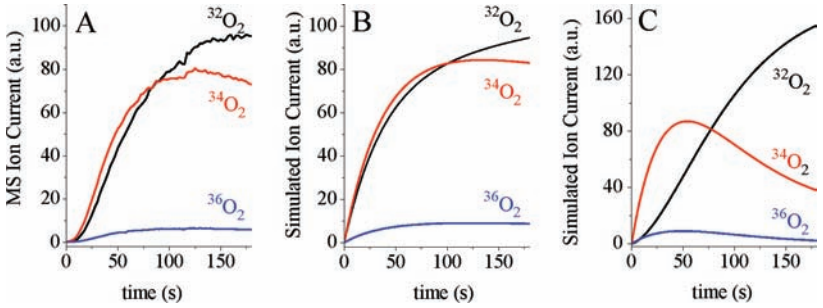

Figure 2. Kinetic traces for the evolution of O_2 isotopes from the $^{18}OH_2$-enriched $[Ru(bpy)_2(OH_2)]_2O^{4+}$ ions. Panel A: Experimental data adapted from ref 5. Panel B: Kinetic simulation based upon concurrent electrophile−nucleophile and two-solvent pathways (Scheme 1) assuming no water exchange between the coordination sphere and solvent ($k_{exch}=0$). Panel C: "Best-fit" simulation based upon the electrophile−nucleophile pathway with simultaneous water exchange ($k_{exch}=2\times10^{-2}$ s^{-1}; $n_1=1$; $n_2=n_3=0$). An experimentally determined value of the turnover rate constant ($k=0.005$ s^{-1})[7] was used for all simulations. The explicit kinetic model used is given in the Supporting Information.

of absolute ethanol to the acid chloride of 4,4′-dicarboxy-2,2′-bipyridine.[22] The complex ions, $Ru(bpy)_3^{2+}$, $Ru(dcb)_2bpy^{2+}$, and $[Ru(bpy)_2(OH_2)]_2O^{4+}$ were prepared by standard procedures[23−26] and isolated as their perchlorate salts. Triflic acid (98% CF_3SO_3H, Alfa Aesar) was vacuum-distilled to remove UV-absorbing impurities and stored at 10 °C as a 2 M solution. Other reagents were the best available grade and used as received; all solutions were prepared in reverse osmosis-deionized distilled water.

Methods. Gases evolved during dimer-catalyzed oxidation of water by Ce^{4+} or in photocatalyzed reactions by $S_2O_8^{2-}$ were continuously monitored by mass spectrometry. The apparatus and methods used have been described in detail;[5] briefly, the reactions were carried out in a ∼8 mL closed chamber containing ∼7 mL of a solution that was fitted with a Lucite plug containing a glass capillary column that extended into the chamber headspace and a 10 mL syringe which acted as a reservoir for the carrier gas (He). Gas was transferred at a rate of ∼1 mL/min into a VG7070EHF mass spectrometer, allowing ∼10 min to conduct each experiment. To initiate the chemical reactions, solutions containing isotopically enriched catalysts in their {**3**,**4**} oxidation state were purged of O_2 with He and mixed by syringe transfer with similarly purged solutions containing a 70−100-fold excess Ce^{4+} ion. The results obtained did not depend upon the order of addition of the reactants; specifically, the addition of concentrated solutions of the complex catalyst in $^{18}OH_2$-enriched water to diluted 0.5 M triflic acid solutions of Ce^{4+} gave the same O_2 isotopomer ratios and kinetic profiles as when concentrated Ce^{4+} was added to previously diluted solutions of the complex ion. The photochemical reactions were initiated by exposure of the reactant solutions to light from a LED bank emitting at 470 nm; this light source generated a photon flux of $\sim2.5\times10^7$ photons s^{-1} cm^{-2} (or a total flux of $\sim10^8$ photons s^{-1}) as measured by ferrioxalate actinometry. The complete reactant solutions typically contained 100 mM phosphate, at a pH of 7.0, 15 mM $K_2S_2O_8$, 225 μM $Ru(bpy)_3^{2+}$ or 190 μM $Ru(dcb)_2bpy^{2+}$, and 85−130 μM {**3**,**4**}. In one set of chemical experiments, 98% $^{36}O_2$ (ION) was deliberately introduced into the reaction chamber to give a final partial pressure of ∼0.2 atm and allowed to equilibrate with the solution prior to starting the chemical reaction. The mass spectrometric data were analyzed as previously described.[5] Briefly, peak intensities measured at various times for mass/charge ratios of 32, 34, and 36 were corrected for background counts (including trace amounts of $^{32}O_2$ present from the atmospheric contamination), and their ratios were then extrapolated to zero time to correct for the time-dependent loss of an isotopic label from the catalyst coordination sphere. From these initial ratios and the known isotopic composition of the reaction components, the relative contributions of the isotopically defined pathways can easily be calculated.

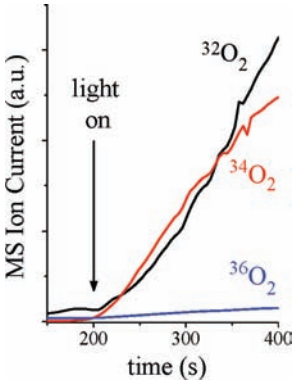

Figure 3. Mass spectrometric traces showing the evolution of O_2 isotopomers during photochemical oxidation of the $^{18}OH_2$-enriched $[Ru(bpy)_2(OH_2)]_2O^{4+}$ ion at 25 °C. Conditions: 125 μM $[Ru(bpy)_2(OH_2)]_2O^{4+}$, 190 μM $Ru(dcb)_2bpy^{2+}$, and 15 mM $K_2S_2O_8$ in 50 mM phosphate buffer (pH 7.0).[17] The arrow indicates the point at which the solution was illuminated at 470 nm.

Optical spectra were measured using a HP 8452A diode array spectrophotometer. Kinetic modeling was made using Berkeley Madonna, version 8.3.9.

Results

Mass Isotopic Distributions of Evolved O_2. In all cases, initiation of catalyzed water oxidation by the direct addition or photochemical generation of strong oxidants led to dramatic increases in the content of $^{32}O_2$ and $^{34}O_2$ in the headspace gases, with considerably smaller amounts of $^{36}O_2$ (comprising at most 7% of the other isotopes) being formed. Time-dependent changes in peak intensities are illustrated for Ce^{4+} oxidations catalyzed by $[Ru^{III}(bpy)_2(OH_2)]_2O^{4+}$ in Figure 2A and for the corresponding $Ru(dcb)_2(bpy)^{2+}$-photoinitiated reaction that used $S_2O_8^{2-}$ as the oxidant in Figure 3. For all reactions, the rates of $^{34}O_2$ formation relative to $^{32}O_2$ slowly decreased over the course of the reaction (typically two to three turnovers), which is consistent with a progressive loss of ^{18}O from the primary coordination sphere of the catalyst. Counts at $m/z = 28$ (N_2) were nearly constant over the course of the reactions, indicating that background

(22) Garelli, N.; Vierling, P. *J. Org. Chem.* **1992**, *57*, 3046–3051.
(23) Sullivan, B. P.; Salmon, D. J.; Meyer, T. J. *Inorg. Chem.* **1978**, *17*, 3334–3341.
(24) Damrauer, N. H.; Boussie, T. R.; Devenney, M.; McCusker, J. K. *J. Am. Chem. Soc.* **1997**, *119*, 8253–8268.
(25) Anderson, P. A.; Anderson, R. F.; Furue, M.; Junk, P. C.; Keene, F. R.; Patterson, B. T.; Yeomans, B. D. *Inorg. Chem.* **2000**, *39*, 2721–2728.
(26) Elliott, M. C.; Hershenhart, E. J. *J. Am. Chem. Soc.* **1982**, *104*, 7519–7526.

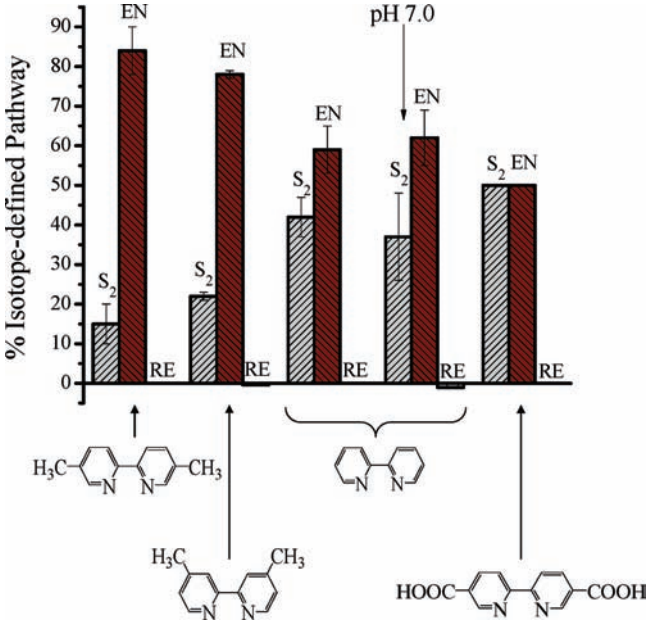

Figure 4. Distribution of O_2 catalysis pathways (Scheme 1) for various $[RuL_2(OH_2)]_2O^{4+}$ ions calculated from initial isotope ratios. Gray bars, two-solvent (S_2) pathway; crimson bars, electrophile−nucleophile (EN) pathway; white bars, intramolecular reductive elimination (RE) pathway. Specific ligands (L) are identified by the structures given below the bar graph. Data for the methyl-substituted bipyridine analogs are averages of duplicate determinations made at 25 °C in 0.5 M CF_3SO_3H; the chemical reactions for the unsubstituted dimer were from a previously reported[5] larger data set at 28 °C in the same medium, and the photochemical data (labeled as "pH 7") are the results for triplicate determinations made using either 190 μM $Ru(dcb)_2bpy^{2+}$ or 225 μM $Ru(bpy)_3^{2+}$ as a photosensitizer with other conditions as given in Figure 3. For reactions of Ce^{4+} with the unsubstituted dimer, $[Ru(bpy)_2(OH_2)]_2O^{4+}] = 0.04-0.86$ mM, for the substituted analogs, $[RuL_2(OH_2)]_2O^{4+}] = 0.25-0.36$ mM, and, in all cases, $[Ce^{4+}] = 25$ mM. Error limits, where applicable, are the average deviation from the mean value. A complication observed in the reactions of the 5,5′-dicarboxybipyridine-containing catalyst was precipitation of a ruthenium-containing product following addition of the Ce^{4+} oxidant.

levels of atmospheric gases were unchanged; the intensities of these peaks were used to correct the $^{32}O_2$ counts for the atmospheric contribution, that is, by assuming that the contaminant $^{32}O_2$ contribution to $m/z = 32$ was 25% of the total N_2 counts. In all cases, counts at $m/z = 44$ (CO_2) were very low and underwent barely detectable increases over the course of the chemical reactions. This behavior parallels our earlier results on the unsubstituted dimer, where Ce^{4+}/catalyst concentration ratios as large as 600-fold were used.[5] Small amounts of CO_2 were also formed during the photochemical generation of O_2. Control experiments indicated that equivalent amounts of CO_2 were formed under illumination when the dimer was absent, and that CO_2 was generated in dark reactions in the absence of both a catalyst and photosensitizer. Thus, the identity of the oxidizable organic material giving rise to these trace levels of CO_2 is unknown but can include only minimal contribution from the catalyst itself. Relative contributions of the three isotopically identifiable pathways (Scheme 1), that is, both O atoms derived from the solvent (S_2), both from the coordination sphere (RE), and one from each environment (EN), are summarized in Figure 4.

Additional studies were made in an environment to which $^{36}O_2$ had been deliberately added to probe for

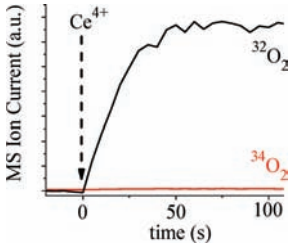

Figure 5. Isotopic composition of O_2 from a reaction of unlabeled {**5**,**5**} in a medium oxygenated with 98% $^{36}O_2$. Conditions: 1.6 mM unlabeled $[Ru(bpy)_2(OH_2)]_2O^{4+}$ in 0.5 M triflic acid, with Ce^{4+} added to a final concentration of 32 mM to promote O_2 evolution. $^{36}O_2$ was enriched in the solution and headspace to a partial pressure of ~0.2 atm as described in the Experimental Section.

possible scrambling of catalyst-generated O_2 with a solvent during reaction. For these reactions, 2−3 mL of 98% $^{36}O_2$ was bubbled from a syringe through a deoxygenated 0.5 M triflic acid solution containing unlabeled {**3**,**3**}; the injected gas was then manually mixed with the He in the reaction headspace and reservoir. This procedure was repeated several times over a 30 min period to give a headspace partial pressure of ~0.2 atm $^{36}O_2$, based upon the amount of gas injected, after which the reaction was initiated by adding excess deoxygenated Ce^{4+} solution. Mass spectrometric analyses of the evolved gases indicated that the amount of $^{34}O_2$ did not increase over a background level of ~3% over the reaction period. During the reaction, $^{36}O_2$ levels also remained nearly constant, although, as expected, $^{32}O_2$ levels increased dramatically (Figure 5). These results exclude the possibility that exchange occurs between O_2 and H_2O during the catalytic oxidation of water. At the later stages of the reaction, a very small peak at $m/z = 46$ was detected, corresponding to the formation of $C^{16}O^{18}O$. The appearance of this species suggests that catalyst-generated O_2 may contribute to decomposition of the organic material, as noted in the preceding parargraph.

Kinetic Modeling. The mass spectrometric data represent kinetic traces of O_2 evolution that can be treated as a flow reactor. As illustrated in Figure 2B, the experimental data can be simulated very closely by a kinetic model (Supporting Information) in which the chemical reaction is assumed to occur by two concurrent pathways involving O_2 formation from two solvent molecules and from one coordinated oxo atom and one solvent molecule, respectively. These calculations make use of a previously determined value for the turnover rate constant ($k = 0.005\ s^{-1}$) for the underivatized catalyst.[7] If other values for k are assumed, the experimental and calculated time scales no longer align, although the relative isotopomer distributions remain unchanged. The requirement that the experimentally determined rate constant be used to achieve quantitative matching of O_2 evolution traces constitutes an important control supporting the premise that water oxidation is indeed catalyzed by the blue dimer.

The data can also be used to test alternative chemical reaction models, for example, one in which the formation of $^{32}O_2$ arises not from an independent redox pathway, but from water exchange in higher oxidation states that occurs concurrently with water oxidation (Scheme 2). In this case, the apparent two-solvent pathway could be ascribed to an accelerated loss of ^{18}O from the coordination

Scheme 2. Water Exchange Mechanism for Isotope Scrambling by the Electrophile−Nucleophile (EN) Pathway

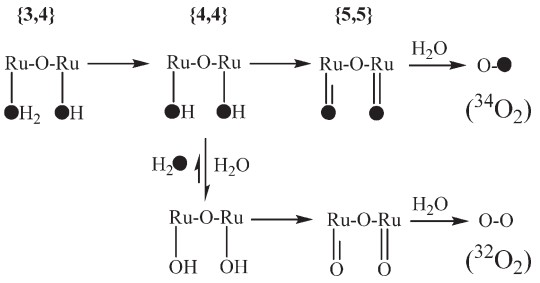

sphere of the complex ion. However, as illustrated in Figure 2C, this type of model cannot account for the reaction profiles observed by mass spectrometry. Specifically, at relatively low exchange rates, there is a pronounced induction period before the onset of $^{32}O_2$ formation, and at relatively high exchange rates, $^{34}O_2$ accumulation is rapidly truncated. This same pattern is observed in calculations that consider an expanded set of elementary reaction steps.

Discussion

Absence of Exchange Mechanisms. An unusual axial signal associated with the {**5**,**5**} oxidation state appears in the $g \sim 2$ region of the cryogenic EPR spectrum during catalytic turnover.[7,8] This signal has properties that suggest substantial ligand radical character,[3,17] including electron−nuclear double resonance and electron spin echo envelope modulation spectra displaying proton hyperfine coupling.[27] We have hypothesized that this signal might be a ligand radical formed by internal one-electron reduction of the Ru^V-O-Ru^V core, such as shown in Figure 1. Given the propensity of the O_2 diradical to couple with carbon-centered radicals to form peroxyl compounds,[28] it seemed worthwhile to consider whether catalyst-generated dioxygen could react with this intermediate (for example, as shown in Scheme 3) to initiate O atom exchange. One possible mechanism for such scrambling could be the well-documented bimolecular decomposition pathways of peroxyl compounds which proceed through tetroxide intermediates formed by radical−radical coupling.[28] Accordingly, we ran the chemical reactions in an atmosphere containing $^{36}O_2$ under conditions where the only product from the catalyzed oxidation pathways would be $^{32}O_2$, that is, using unlabeled {**3**,**3**}. Under these conditions, any $^{34}O_2$ that formed must arise from O scrambling and would be easily detected in the product mass spectra. The observation that negligible $^{34}O_2$ accumulated (Figure 5) clearly establishes the absence of O_2-H_2O exchange by any pathway in this reaction and, therefore, that the copious amounts of $^{32}O_2$ formed during the reaction with the [^{18}O]-H_2O labeled complex (Figures 2A and 3) cannot be an artifact arising from this source.

(27) Unpublished observations by Michael K. Bowman (University of Alabama) and Jamie Stull and David Britt (University of California at Davis).

(28) von Sonntag, C. *The Chemical Basis of Radiation Biology*; Taylor and Francis: London, 1987; pp 65−77.Breen, A. P.; Murphy, J. A. *Free Radic. Biol. Med.* **1995**, *18*, 1033–1077. Cadet, J.; Berger, M.; Buchko, G. W.; Joshi, P. C.; Raoul, S.; Ravanat, J.-L. *J. Am. Chem. Soc.* **1994**, *116*, 7403–7404.

Scheme 3. Hypothetical Pathway for O_2 Addition to a Ligand Radical Intermediate Leading to Isotope Scrambling

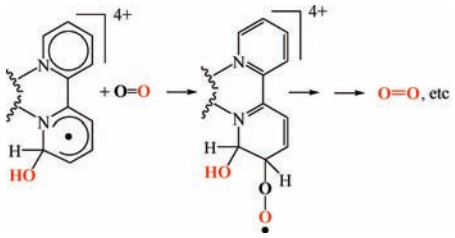

Likewise, a loss of the label through water exchange could lead to the formation of more $^{32}O_2$ than predicted by the pathway involving O−O bond formation between a coordinated oxo atom and H_2O (Scheme 2) and thereby give the appearance of another redox pathway where none existed. Water exchange on {**3**,**4**} has been directly measured[21] and is too slow to contribute to exchange at the coordination site. Although exchange on {**3**,**3**} does occur on time scales comparable to O_2 evolution, the amount of {**3**,**3**} present at the redox poises of these experiments is negligible,[17] and therefore this reaction also contributes negligibly to exchange.[21] However, {**4**,**4**} and {**4**,**5**} accumulate during turnover in acidic[7] and neutral media,[6,19] respectively, and their water exchange dynamics have not been directly measured. It is highly unlikely from both crystal field arguments and the fact that the aqua ligands are deprotonated in {**4**,**4**} and {**4**,**5**} that exchange would occur more rapidly on these ions than on {**3**,**3**}. Specifically, {**4**,**4**} contains low-spin d^4 ruthenium centers, and {**4**,**5**} contains formally low-spin d^4 and d^3 centers, although the latter may have significant d^4 character.[1,9] For both associative and dissociative pathways, the contribution of crystal field activation energies is predicted to be greater for these centers than for the low-spin d^5 centers in {**3**,**3**}.[29] In acidic solutions, {**3**,**3**} exists as the diaqua complex,[20] whereas {**4**,**4**} is dihydroxy[30] and {**4**,**5**} is dioxo ligated.[19,30] Thus, energetically unfavorable protonation and attractive electrostatic forces would contribute to the activation barrier for exchange in {**4**,**4**} and {**4**,**5**}, but not in {**3**,**3**}.[31] Consequently, the exchange rate constant measured for {**3**,**3**}, $k_{ex} = 7 \times 10^{-3}$ s^{-1} (at pH 0.3, 25 °C),[21] is a conservative upper limit for the actual exchange rate constants for the higher oxidation states. Even with the assumption of a value that is $3 \times k_{ex}$ (Figure 2C), the simulations exhibit profiles that are totally unlike the experimentally determined kinetic profiles for evolution of the individual isotopes (Figure 2A). This incongruence is intuitively reasonable. If the appearance of $^{32}O_2$ relied upon water exchange in the coordination site following initiation of the reaction, then there would exist either a pronounced induction period for the appearance of $^{32}O_2$ relative to $^{34}O_2$ or, at faster water exchange rates, a rapid loss of the label from the aqua site would severely curtail the $^{34}O_2$ yield within the first turnover of the catalyst. The calculated traces in Figure 2C represent a compromise between

(29) Basolo, F.; Pearson, R. G. *Mechanisms of Inorganic Reactions*, 2nd ed.; Wiley: New York, 1967.

(30) Cape, J. L.; Lymar, S. V.; Lightbody, T.; Hurst, J. K. *Inorg. Chem.* **2009**, *48*, 4400–4410.

(31) Lundberg, M.; Blomberg, M. R. A.; Siegbahn, P. E. M. *Theor. Chim. Acc.* **2003**, *110*, 130–143.

these extremes, from which it is evident that mechanisms involving water exchange at the cis-aqua coordination site are fundamentally incapable of reproducing the experimental data. It is also clear from these results that the absence of appreciable formation of $^{36}O_2$ cannot be ascribed to a rapid exchange of water under catalytic conditions that masks coupling and reductive elimination of coordinated oxo atoms by intramolecular or bimolecular pathways (Scheme 1). Specifically, it is inconceivable that a rapid loss of only one coordinated water, leading to an inappreciable formation of $^{36}O_2$, could occur without a loss of the second, which would necessarily lead to an inappreciable formation of $^{34}O_2$ as well, in contrast with the experimental results (Figures 2A and 3).

The reaction of Ce^{4+} with $[(bpy)_2Ru(OOH)ORu(OH)(bpy)_2]^{4+}$ or a similar peroxo intermediate formed by reaction of the $[Ru(=O)_2]O$ core in {**5**,**5**} might also lead to the formation of $^{32}O_2$ if the reaction proceeded by coupling of a ceric-coordinated water ligand with the terminal peroxo O atom. Subsequent cleavage of the peroxo O−O bond, rather than the Ru−O bond, would lead to a net formation of O_2 from two solvent molecules with the ^{18}O label remaining in the Ru coordination sphere. However, $^{32}O_2/^{34}O_2$ ratios measured for the photochemically driven reactions at pH 7 were indentical within experimental uncertainty (Figure 4). For these latter reactions, which made use of $Ru(bpy)_3^{3+}$ analogs and $SO_4^{\bullet-}$ as oxidants, it is difficult to imagine this sort of coupling occurring at all, much less with the same selectivity as Ce^{4+}. Consequently, reaction models that are independent of the oxidant identity are inherently more appealing.

Comparisons with Other Proposed Mechanisms. The failure of these alternative mechanisms to account for the data strongly suggests that a bona fide pathway does exist for O−O bond formation from two solvent molecules. Whatever its nature, this pathway is apparently quite general for this class of catalysts, since it is observed for several bipyridine analogs and in media with widely varying compositions (Figure 4). We have adapted the extensive literature on covalent hydration[15] and pseudobase formation[16] by nitrogen heterocycles and concepts developed from studies on $M(bpy)_3^{3+}$ decomposition in basic solutions[12−14] and other reactions of coordination complexes[32] to suggest a pathway involving noninnocent participation of the bipyridine ligands (Figure 1). As noted in the Introduction, we have amassed data that are consistent with this mechanism; none of this is definitive, however. For example, the radical signals and NIR bands that are diagnostic of $OH^{\bullet}$ addition to the ring could be associated with "dead end" species in equilibrium with the active form of the catalyst.[17]

An alternative mechanism involving expansion of the Ru primary coordination sphere by the addition of H_2O,[33] which then reacts with a second water molecule, is difficult to exclude. Recent combined experimental and DFT theoretical studies examining water oxidation catalyzed by mononuclear polypyridyl Ru^{II} complexes that lack coordinated water have supported just such a mechanism.[34] In this proposed mechanism, oxidation to Ru^{IV} is followed by H_2O addition, after which the seven-coordinate complexes undergo further two-electron oxidation with a loss of protons to give $L_6Ru^{VI}=O$ species that react with H_2O to form peroxo-bound intermediates. Electronic rearrangement then leads to the release of O_2 and regeneration of the catalyst in its original (Ru^{II}) oxidation state. The turnover rate constants for these catalysts calculated from the reported data are $k_{cat} \leq 4 \times 10^{-2}$ s^{-1} at 20 °C, in 0.1 M triflic acid, which is an order of magnitude greater than the overall value for {**5**,**5**} measured in 0.5 M triflic acid ($k_{cat} \approx 5 \times 10^{-3}$ s^{-1}).[5] In these studies with mononuclear complexes, initial rates within homologous series increased with increasing electron donation from bipyridine substituents, which is opposite to the fractional order of contribution from the two-solvent pathway reported here for the dinuclear catalyst (Figure 4). The order observed for the μ-oxo dimers is consistent with a pathway involving "covalent hydration" of the bipyridine ligands, a reaction which is promoted in other nitrogen heterocycles by electron withdrawal from heterocyclic rings and retarded by steric constraints at potential binding sites imposed by the substituents.[15] Correspondingly, both factors should disfavor this pathway in the methylated derivatives but have opposing effects in the carboxylated derivative, which is consistent with the observed pattern (Figure 4). One additional consideration bearing on these mechanisms is the absence of water exchange during catalytic turnover of the dimer. Specifically, it is difficult to imagine a mechanism where expansion of the ruthenium coordination sphere by H_2O would not also lead to measurable exchange with the coordinated aqua ligand in these catalysts, particularly when {**5**,**5**} decomposition is rate-limiting.[4,5] Finally, we note that recent theoretical modeling studies of the "Tanaka catalyst",[35] a dimeric ruthenium complex containing cis-oriented aqua ligands, suggest that O_2 formation occurs via redox cycling of the electroactive benzoquinone ligands without altering the oxidation states of bound Ru^{II} ions.[36] This electrocatalyst may therefore represent an extreme example of noninnocent ligand participation in water oxidation.

The pathway for water oxidation catalyzed by another dinuclear Ru complex ion,[37] *cis*,*cis*-$[Ru^{II}(trp)(OH_2)]_2(\mu\text{-bpp})^{3+}$ (where trp = 2,2′:6,2″-terpyridine and bpp = 2,6-bis(pyridyl-pyrazolate)) has recently been determined by ^{18}O-isotopic labeling studies.[38] This ion differs from the "blue dimer" in having a pyrazolate bridging ligand in place of an oxo atom and having stable redox states between {**2**,**2**} and {**4**,**4**}. Both experimental data and DFT calculations[39] indicate that the highest oxidation state has a $[Ru(=O)]_2L$ core and is the only oxidation state capable of evolving O_2. Selective ^{18}O-labeling of the

(32) Sagüés, J. A. A.; Gillard, R. D.; Lancashire, R. J.; Williams, P. A. *J. Chem. Soc., Dalton Trans.* **1979**, 193–198. Gillard, R. D. *Coord. Chem. Rev.* **1975**, *16*, 67–94.
(33) Serpone, N.; Ponterini, G.; Jamieson, M. A.; Bolletta, F.; Maestra, M. *Coord. Chem. Rev.* **1983**, *50*, 209–302.
(34) Tseng, H.-W.; Zong, R.; Muckerman, J. T.; Thummel, R. *Inorg. Chem.* **2008**, *47*, 11763–11773.
(35) Wada, T.; Tsuge, K.; Tanaka, K. *Inorg. Chem.* **2001**, *40*, 329–337.
(36) Muckerman, J. T.; Polyanski, D. E.; Wada, T.; Tanaka, K.; Fujita, E. *Inorg. Chem.* **2008**, *47*, 1787–1802.
(37) Sens, C.; Romero, I.; Rodriguez, M.; Llobet, A.; Parella, T.; Benet-Buchholz, J. *J. Am. Chem. Soc.* **2004**, *126*, 7798–7799.
(38) Romain, S.; Bozoglian, F.; Sala, X.; Llobet, A. *J. Am. Chem. Soc.* **2009**, *131*, 2768–2769.
(39) Yang, X.; Baik, M.-H. *J. Am. Chem. Soc.* **2008**, *130*, 16231–16240.

coordinated water molecules has established that the primary pathway for O_2 formation is intramolecular reductive elimination of coordinated oxo atoms, that is, the pathway in which both O atoms are obtained from the coordination sphere of the complex ion (Scheme 1).[38] Interestingly, DFT analyses of reaction coordinates had predicted that intramolecular O−O bond formation between the adjacent ruthenyl oxo atoms would be energetically favorable, but that release of O_2 from the 1,2-μ-peroxo-bridged Ru_2^{III} species that formed should be energetically prohibitive.[39] In this scheme, this transient species was therefore viewed as a "dead-end" complex. An alternative low-energy pathway was found that involved protonation of one of the ruthenyl oxo atoms, followed by two-electron oxidation of water at the other ruthenyl oxo to form a terminally bound peroxo group.

In any event, catalytic pathways in the "blue dimer", where intramolecular coupling of ruthenyl oxo atoms does not occur (Scheme 1, Figure 4),[5] contrast markedly with those for the Tanaka and Llobet catalysts, where coupling is apparently facile.[36,38] These mechanistic differences undoubtedly can be attributed in large part to the respective molecular structures. Internuclear separation distances between the oxo atoms in {**5**,**5**} are calculated to be ~4.5 Å,[3,19] whereas they are ~2.1 Å in the Llobet catalyst[37] and ~2.6 Å in the Tanaka catalyst,[38] requiring considerably less molecular distortion to form an internal O−O bond.

Acknowledgment. The authors thank Professor Gary Brudvig (Yale University) for suggesting the potential involvement of the Ce^{4+} ion in $^{32}O_2$ formation. This research was supported financially by the Chemical Sciences, Geosciences, and Biosciences Division, Office of Basic Energy Sciences, Office of Science, U.S. Department of Energy under Grant No. DE-FG02-06ER15820.

Supporting Information Available: The kinetic model used to construct Figure 2B,C and representative traces obtained with various assumptions concerning water exchange rates. This material is available free of charge via the Internet at http://pubs.acs.org.